Curr Radiol Rep (2016) 4:53
DOI 10.1007/s40134-016-0179-3

PET/CT IMAGING (R MORGADO, SECTION EDITOR)

The Role of PET/CT in the Assessment of Primary Bone Tumors

Julio Brandao Guimaraes[1,2,3] · Luca Facchetti[1] · Leticia Rigo[2] · Diego Lessa Garcia[2,3] · Pricila Gama[2] · Benjamin L. Franc[1] · Lorenzo Nardo[1]

Published online: 18 August 2016

Abstract
Purpose of review The purpose of this article is to provide an overview of primary bone malignancies and the role of PET/CT in their diagnosis, staging, and follow-up.
Recent findings PET/CT provides both anatomic and metabolic data; for this reason, the technique has been increasingly used to characterize, stage, and follow up bone lesions.
Summary PET/CT can be performed using different radiotracers and different techniques. Here, the application of single whole-body 18F-FDG and 18F-NaF PET as well as the acquisition methods for characterizing bone tumors is reviewed.

Keywords PET/CT · Primary bone tumors · Osteosarcoma · Chondrosarcoma · Fibrous dysplasia · Multiple myeloma

This article is part of the Topical Collection on *PET/CT Imaging*.

✉ Julio Brandao Guimaraes
Julio.BrandaoGuimaraes@ucsf.edu;
juliobrandaoguimaraes@hotmail.com

Luca Facchetti
Luca.Facchetti@ucsf.edu

Leticia Rigo
letirigo3@hotmail.com

Diego Lessa Garcia
diegoalg@yahoo.com.br

Pricila Gama
pgama.med@gmail.com

Benjamin L. Franc
Benjamin.Franc@ucsf.edu

Lorenzo Nardo
Lorenzo.Nardo@ucsf.edu

[1] Department of Radiology and Biomedical Imaging, University of California UCSF, San Francisco, 185 Berry St, Suite 350, San Francisco, CA 94158, USA

[2] Department of Radiology and Nuclear Medicine, Hospital Beneficencia Portuguesa de Sao Paulo, Sao Paulo, Brazil

[3] Department of Radiology, Federal University of Sao Paulo, UNIFESP, Sao Paulo, Brazil

Introduction

The purpose of this article is to provide an overview of primary bone malignancies and the role of nuclear medicine in their diagnosis, staging, and follow-up.

Primary malignant bone tumors are relatively rare with an incidence of 1 new case per 100,000 men and women per year and a lifetime risk of developing of approximately 0.1 % [1].

Radiologic Approach to Characterizing Bone Tumors

The radiological diagnosis of bone tumors is complicated by their many histologic types and variants, important considerations when choosing treatment options. While there is a wide histologic spectrum of malignant primary bone tumors [2], only a few types account for more than 90 % of bone tumors: osteosarcoma (the most common), chondrosarcoma, Ewing sarcoma, chordoma, and malignant fibrous histiocytoma.

Using a systemic approach including patient age, lesion location, pattern of destruction, matrix, and distribution can help radiologists in the differential diagnosis. Considering age, for example, eosinophilic granuloma and lymphoma are more likely to appear in young children, osteosarcoma and Ewing's sarcoma more frequently present between the

ages of 5–30, and chondrosarcoma, fibrosarcoma, multiple myeloma, and metastases are generally limited to adults. Based on location, eosinophilic granuloma, Paget's disease, plasmacytoma, and bone metastases are often seen in the skull; osteosarcoma, osteochondroma, chondrosarcoma, and fibrosarcoma are usually seen in the long bone metaphysis, while Ewing's and lymphoma are seen in the diaphysis. Typical epiphyseal lesions are chondroblastoma, eosinophilic granulomas, and giant cell tumors (arising from the metaphases). Osteoid osteoma is a cortical lesion. The matrix of the lesion is very helpful in its diagnosis: an ivory, fluffy matrix is typical of osteoid lesions such as osteochondroma and osteoblastoma; ring and arcs are seen in the setting of tumor with a chondroid matrix such as chondrosarcoma or enchondroma; ground-glass appearance is hallmark of fibrous dysplasia. Based on the pattern of bone destruction (Fig. 1), lymphoma and Ewing's sarcoma are more likely to be permeative, while metastases and multiple myeloma tend to have a moth-eaten appearance. Lastly, a polyostotic or monostotic distribution might be the main clue to reach the correct diagnosis; fibrous dysplasia, metastases, multiple myeloma, enchondroma, and brown tumors are often seen involving multiple different locations of the skeleton.

Role of 18F-FDG PET/CT in Characterizing Bone Tumors

On top of these clinical and anatomical features, the metabolic rate of a tumor is another critical parameter in the assessment of bone tumors [3]. Malignant tumors are associated with increased glycolysis compared to normal tissues, likely related to increased number of GLUT transporters and a higher concentration of hexokinase within malignant cells. As a glucose analog, 18F-FDG is transported into cells by surface GLUT-1 transporters and then incorporated into the cell where it is phosphorylated and trapped.

In the past 10 years, the use of 18F-FDG PET/CT has increased given its potential to detect metabolic changes in the tissue, even before the onset of anatomic changes. A full review of the literature performed in the meta-analysis study of Bastiaannet et al. [4] demonstrated that 18F-FDG PET/CT has high sensitivity and specificity in discriminating between sarcomas and benign tumors, and low- and high-grade sarcomas based on the semiquantitative measurements of the glucose consumption. However, at the present time, the American College of Radiology appropriateness criteria guideline [5] does not recommend the use of PET/CT in the staging or characterization of primary bone tumors, in part likely because of the overlap in the range of SUVs between benign and malignant lesions. Nevertheless, PET/CT is felt to be an extremely useful tool for many orthopedic oncologists, who are increasingly referring patients for PET/CT for its high sensitivity (>80 % [6, 7]) in the detection of bone metastases and recurrence. In addition, interest in dual-phase PET/CT has grown recently. This modality aims to distinguish different tissues based on their different 18F-FDG uptake kinetics: malignant lesions continually increase their uptake of radiotracer, while benign conditions usually are characterized by increased uptake on the early-phase, but decreased or monotonic uptake on delayed-phase images [8•]. Multiple studies have demonstrated that the comparison between early- and delayed-phase uptake can help distinguish benign from malignant tissues [9–11].

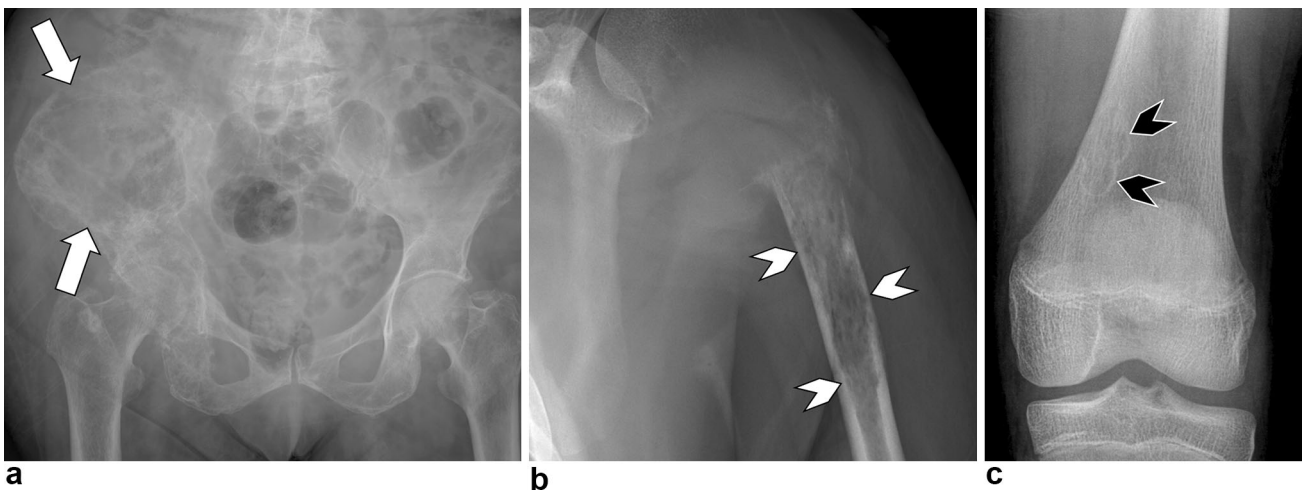

Fig. 1 Patterns of bone destruction: **a** moth-eaten (*white arrows*), **b** permeative (*white arrowheads*), and **c** geographic (*black arrowheads*)

Role of 18F-NaF PET/CT in Characterizing Bone Tumors

18F-NaF has been available for many years but has recently been rediscovered as the application of PET has grown. This radiotracer has a similar distribution to the single-photon-emitting 99mTc-MDP used in general nuclear bone scan imaging but has the advantage of improved image resolution and faster image acquisition time afforded by PET. In the spectrum of primary bone tumors, one of the main indications for PET/CT with 18F-NaF is in the assessment of osteosarcoma. Usually, 18F-NaF has higher specificity compared to FDG in localizing sclerotic bone lesions, but has inferior performance in the assessment of lytic bone lesions. For this reason, the combined use of NaF and FDG has been studied with initial success [12, 13•].

In the remainder of this review, we will describe the main radiological characteristics of primary bone tumors with particular attention to their features on PET/CT.

Osteoblastic Tumors

Osteosarcoma

Osteosarcoma (OS) is the most common primary malignant bone tumor in children and adolescents [14], and it is the second most common primary malignant bone tumor following multiple myeloma in all age groups [15, 16]. OS is more common in males than in females and usually presents as a painful mass rising at the level of the metaphyseal regions, with the knee being the most common site.

Osteosarcomas can be divided into a number of subtypes according to the degree of differentiation, location within the bone (intramedullary, surface/juxtacortical, extraskeletal), and histological variants. Osteosarcoma may also occur as a secondary lesion in association with underlying benign conditions (secondary osteosarcoma).

The most common subtype of OS is the conventional type (80 %). Typical x-ray features include medullary and cortical bone destruction, wide zone of transition, permeative or moth-eaten appearance, aggressive periosteal reaction (sunburst type, Codman triangle, lamellated-onion skin-reaction (Fig. 2), soft tissue mass with variable calcified and osteoid tumor matrix.

The role of CT is usually staging or identification of predominantly lytic lesions in which small amounts of mineralized material may be inapparent on both plain film and MRI. Chest CT is the most appropriate exam (ACR = 9) for the screening of pulmonary metastases from sarcoma. A joint-to-joint MRI is the most accurate study for local staging, particularly in evaluating for intraosseous tumor extension, soft tissue involvement, or skip metastases (ACR = 9). The assessment of the growth plate is essential as up to 75–88 % of metaphyseal tumors do cross the growth plate into the epiphysis. On MRI imaging, the non-mineralized soft tissue component shows intermediate T1w and high T2w signal intensity, while the mineralized/ossified components show low T1 and T2 signal intensity. Scattered regions of hemorrhage with variable signal or of necrosis are also frequent. Evaluation for enhancement of the solid tumor component is essential for guiding biopsy (Fig. 3).

Currently, 18F-FDG PET/CT in osteosarcoma is not considered appropriate by ACR criteria (score <6); however, multiple studies have demonstrated that PET/CT can provide useful information regarding the primary site, staging, and follow-up [17, 18]. As to the primary site, beyond locoregional extent assessment, 18F-FDG PET/CT can assist in estimating the biological aggressiveness of the tumor. High-grade sarcomas are characterized by intense 18F-FDG avidity; in addition, the tumor is often metabolically non-homogeneous and PET/CT may increase the diagnostic yield of biopsy by directing the needle to the area of most intense metabolism [19]. Using a tumor-to-background 18F-FDG uptake cut-off level of 3.0 for malignant bone lesions, according to Schulte et al. [20] the sensitivity (SS), specificity (SP), and accuracy of 18F-FDG PET in identifying malignant OS were 93, 66.7, and 81.7 %, respectively. Furthermore, 18F-FDG PET/CT yields a more accurate preoperative staging of sarcomas than conventional imaging [21, 22]. The accuracy in the characterization of lesions as benign or malignant may be further improved using the dual-phase PET/CT technique because the different kinetic of the benign and malignant tumor. Scanning patient at different time points after injection, the difference of uptake can be used to differentiate benign versus malignant lesions [8].

PET/CT also plays a role in assessing response to treatment and has prognostic significance [23] (Fig. 4). The amount of necrosis induced by neoadjuvant chemotherapy is a significant prognostic factor for survival [8]. Gaston et al. [24] found that a post-therapeutic maximum standardized uptake value of less than 2.5 is predictive of tumor necrosis in osteosarcoma [25]; similarly, Cheon et al. [26] reported that a SUVmax <2 after neoadjuvant chemotherapy correlated with a good histologic response, while values greater than 5 were associated with a poor histologic response.

There are also scattered reports related to the use of 18F-NaF PET/CT in OS, particularly in the assessment of skip lesions or bone metastases [27] (Fig. 5). Another potential application of 18F-NaF PET/CT is in the differentiation between postoperative changes and tumor recurrence after surgery. Unlike 18F-FDG, 18F-NaF does not localize to areas of inflammation but only to newly mineralized bone.

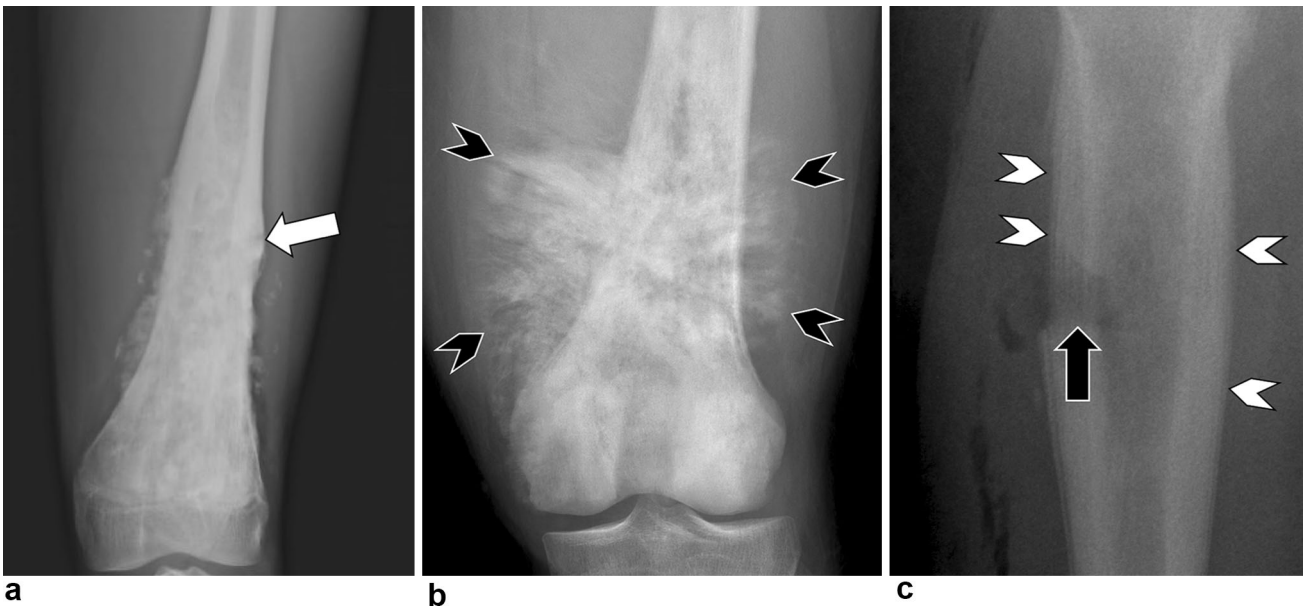

Fig. 2 Patterns of periosteal reaction: **a** Codman's triangle (*white arrow*), **b** sunburst (*black arrowheads*), and **c** onion skin (*white arrowheads*); status post-biopsy (*black arrow*)

Fig. 3 An 18-year-old female, suffering from stiffness and swelling in her right distal thigh for an osteoblastic osteosarcoma grade III **a** AP and LL radiographs showing an aggressive lesion with osteoid matrix and sunburst periosteal reaction (*arrows*) at the level of the distal femoral diaphysis. **b** MRI (axial T2w STIR, T1w, T1w FS +C, DWI B0, DWI B600, DWI ADC-map): enhancing mass arising from the distal diaphysis with intermediate—high SI on T2w and intermediate—low SI on T1w sequence (*white arrow*). A necrotic area is characterized by a very high SI on T2 and no enhancement (*black arrows*). The mass has mild diffusion restriction, while the necrotic area shows a high SI on the DWI images for the T2-shine-through effect (*black arrowhead*). **c** Coronal MRI T1w sequence and bone scan: there is an extensive associated abnormal marrow signal within the right femur extending proximally from the level of the mass to the level of the lesser trochanter (*white arrowheads*), well shown on both the exams

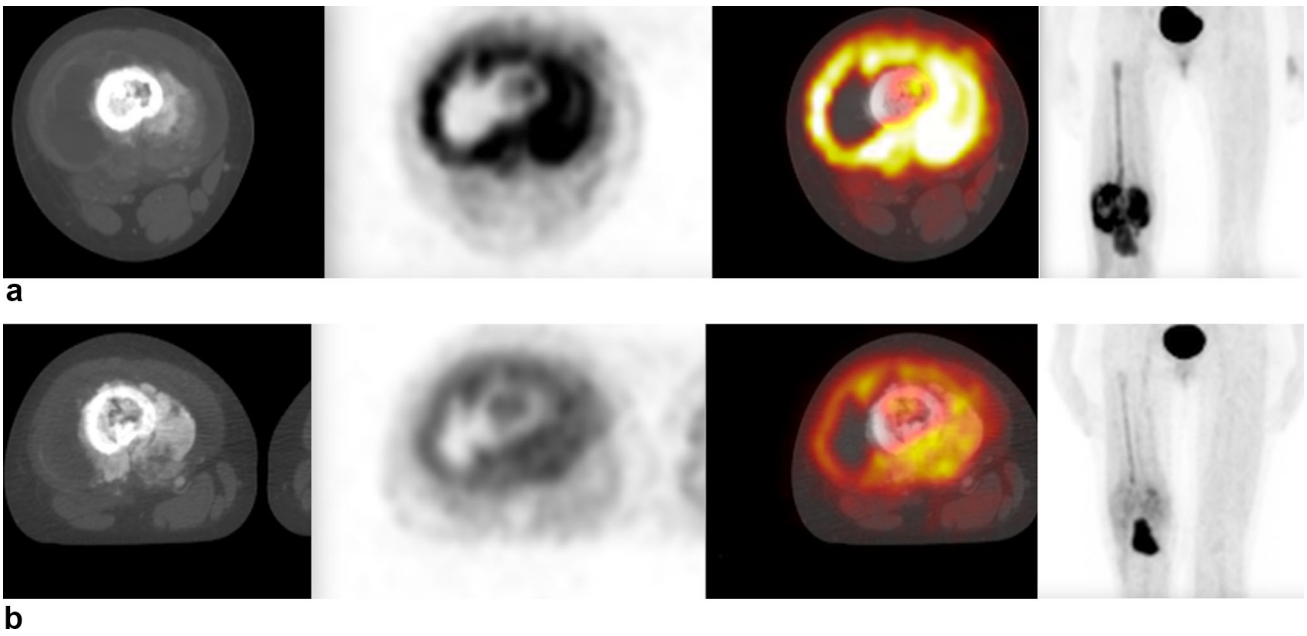

Fig. 4 An 18-year-old female suffering from osteosarcoma; FDG PET/CT at baseline (**a**) and after (**b**) two-month neoadjuvant chemotherapy with adriamycin–cisplatin prior to surgical resection. There is a marked interval decrease in FDG avidity of the enhancing soft tissue mass arising from the right distal femoral metadiaphysis and extending to the proximal metaphysis

However, at the present time there are no definite recommendations for routine use of 18F-NaF PET/CT in osteosarcoma.

Osteoma Osteoid and Osteoblastoma

Osteoma osteoid (OO) and osteoblastoma (OB) usually affect adolescents and young adults [28]. OO is commonly diagnosed in the cortex of the long bones (50 % within the femur or tibia) as an intracortical nidus associated with a variable amount of mineralization, accompanied by cortical thickening and reactive sclerosis in a long bone shaft [29, 30].

OB is more commonly in the posterior element of the spine, with higher incidence in the cervical spine [31]. The differential diagnosis between OO and OB was previously based on a size criterion (1.5-cm nidus); however, more recently OO and OB have been recognized as two different pathologies rather than the differential expression of a single tumor [32]. In fact, OB has a greater potential for growth, with destruction of bone tissue or even malignant transformation, and recurs more often than OO.

X-ray are usually the first imaging study obtained. CT or MRI is used for further characterization. CT scan can demonstrate the sclerotic lesion and the nidus, while MRI can better see intramedullary and soft tissue changes. Bone scan shows intense osteoblastic activity in the tumoral region [33, 34]. There is no specific role for PET/CT in the characterization of OO or OB (Fig. 6); however, PET/CT scan can be used to assess treatment response [35]. For example, PET/CT can be used to monitor radioablation response: efficacy of treatment corresponds to a significant decrease in FDG uptake [36]. Tumor recurrence/persistency can be detected by focal increased radiotracer activity.

Cartilaginous Bone Tumor

The diagnosis of cartilaginous tumors is based on clinical examination and imaging findings. There is a wide spectrum of cartilaginous tumors, ranging from benign tumors without metastatic potential such as enchondroma and osteochondroma to high-grade malignant tumors such as chondrosarcoma with aggressive behavior and early metastases. Multimodality radiologic assessment is mandatory to understand the behavior of the lesion. The x-ray are usually the first diagnostic study obtained; however, often they are not able to fully characterize the lesion and further evaluation with cross-sectional imaging is warranted. CT images can better assess the cartilaginous matrix (arc-and-ring or stippled morphology) and the endosteal scalloping, which might be useful to distinguish enchondroma from a low-grade chondrosarcoma. Enchondroma presents no areas or small areas of endosteal scalloping and usually shows extensive matrix mineralization, while low-grade chondrosarcoma typically shows deep and extensive endosteal scalloping but more limited matrix

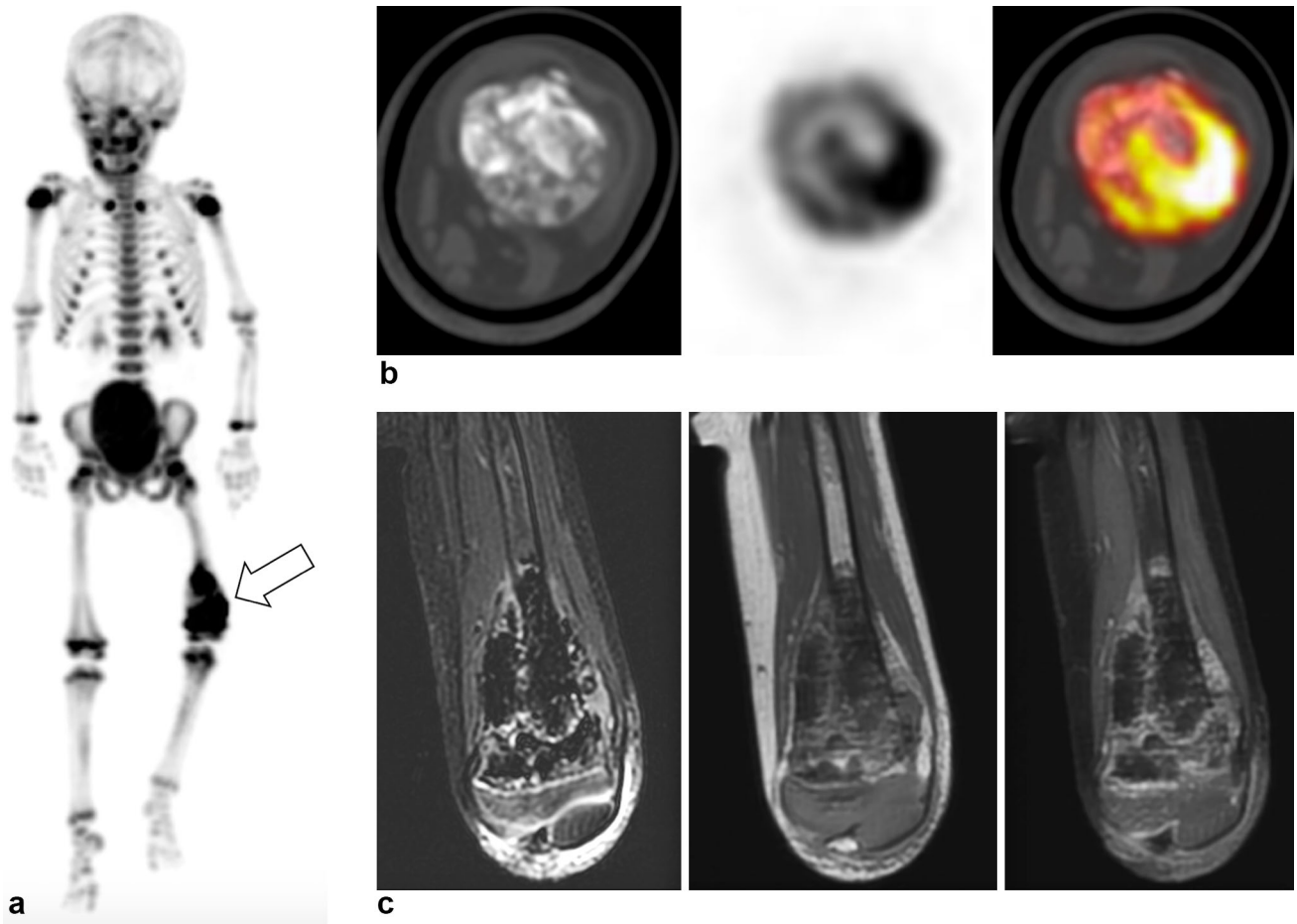

Fig. 5 A 3-year-old male with high-grade osteosarcoma of the left knee. **a** 18F-NaF PET/CT (*MIP images*): the lesion demonstrates intense radiotracer uptake (arrow). **b** 18F-Naf PET/CT (axial CT, PET, PET/CT fused reconstructions) and **c** MRI (coronal T2w STIR, T1w, T1w FS +C) show a heterogeneous mass arising from the distal femoral metaphysis with associated cortical destruction and soft tissue extension. Cast is noted, due to a pathologic fracture

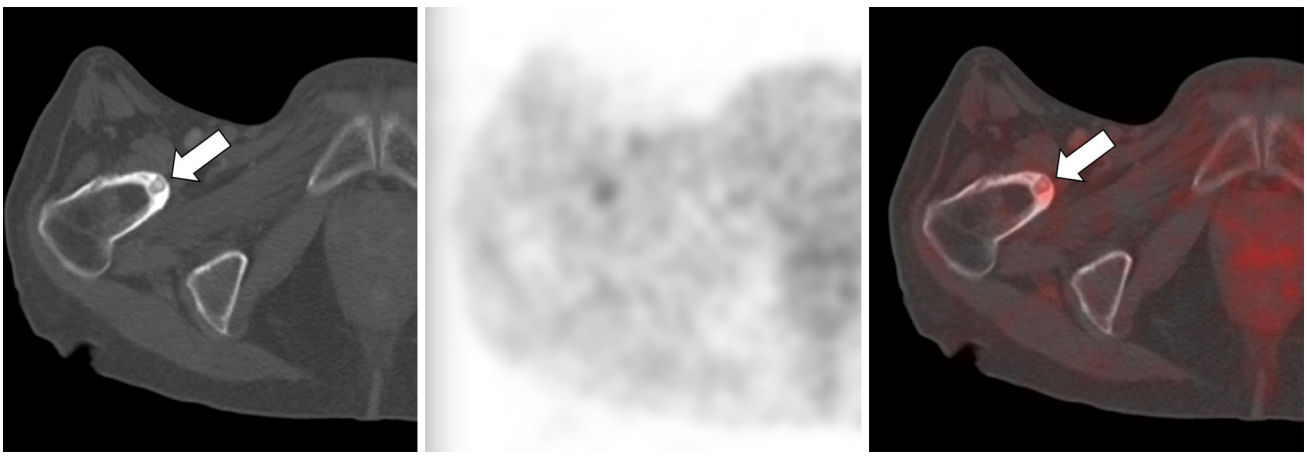

Fig. 6 A 73-year-old male with history of follicular lymphoma. The PET/CT shows an FDG-avid focally lucent nidus within surrounding sclerotic reacting bone and central sclerotic dot (*arrow*) at the level of the right femoral neck. These findings are consistent with osteoid osteoma

mineralization. MRI characteristics of hyaline cartilage include low or intermediate signal on T1-weighted images and high signal on T2 sequences [37] (Fig. 7). The high tissue resolution, especially when gadolinium is administrated, allows for the detection of subtle soft tissue extension of the tumors, strongly favoring malignant etiology.

Both MRI and CT have been demonstrated to be accurate in differentiating osteochondroma from chondrosarcoma by measuring the thickness of the cap, which is usually greater than 2 cm in malignant lesions. Also nuclear medicine bone scan can contribute to the differentiation of benign from malignant lesions, the latter accumulating more 99mTc-MDP [38]. Furthermore, the intrinsic metabolism of cartilaginous tumor can be used as a parameter to distinguish benign from malignant lesions; 18F-FDG PET supplies a functional criterion with which to further assess or supplement morphologic imaging and histopathology. In particular, a SUV greater than 2 has been suggested as a threshold for malignant etiology. Feldman et al. [39] studied a large cohort of cartilage tumors and their data support a correlation between metabolic activity and histology: benign lesions had low SUVs, benign lesions with atypical histological features had slightly higher values, and malignant lesions had SUVs markedly higher than benign lesions (Figs. 8, 9). The work of Aoki et al. [40, 41] supported the use of 18F-FDG PET as an objective tool in differentiating chondrosarcoma from enchondroma and osteochondromas as well as for assessing the grade of chondrosarcomas.

Fibrous Lesions

Fibrous dysplasia (FD) is a benign disorder characterized by proliferation of mesenchymal tissue replacing the trabecular bone with abnormal fibro-osseous tissue. The process is monostotic in the majority of cases; however, about 10–15 % of cases are polyostotic, especially when associated to genetic syndromes such as McCune Albright's or Mazabraud's syndromes. The polyostotic form is often unilateral or monomelic [42].

FD presents in children or young adult as a painless osseous abnormality affecting ribs (28 %), femurs (23 %), or neurocranium (20 %). The amount of woven bone and fibrous tissue determines the x-ray and CT appearance which can be sclerotic, cystic, or mixed cystic–sclerotic [43, 44]. Given its variability of appearance, MRI is usually less useful for the diagnosis. 18F-FDG PET/CT can be useful in the assessment of the extent of the polyostotic form: the bone abnormalities seen as ground-glass, mixed sclerotic, and lytic expansive lesions correspond to increased uptake on the PET images [45]. Multiple authors have described the use of FDG PET/CT in the assessment of rare syndromes associated with FD [46, 47]. In those cases, the technique is also a valuable tool to assess for other abnormalities associated with the specific syndrome, for example intramuscular myxomas in Mazabraud's syndrome. Furthermore, 18F-FDG PET/CT can detect malignant degeneration [48]. FD can degenerate into malignancies (1–4 % cases) such as osteosarcoma, fibrosarcoma, and malignant fibrous histiocytoma, especially in the polyostotic form [49]. In case of progressively increasing 18F-FDG uptake, malignant degeneration should be suspected and a biopsy should be performed using PET/CT guidance [16]. In previous reports, FD was

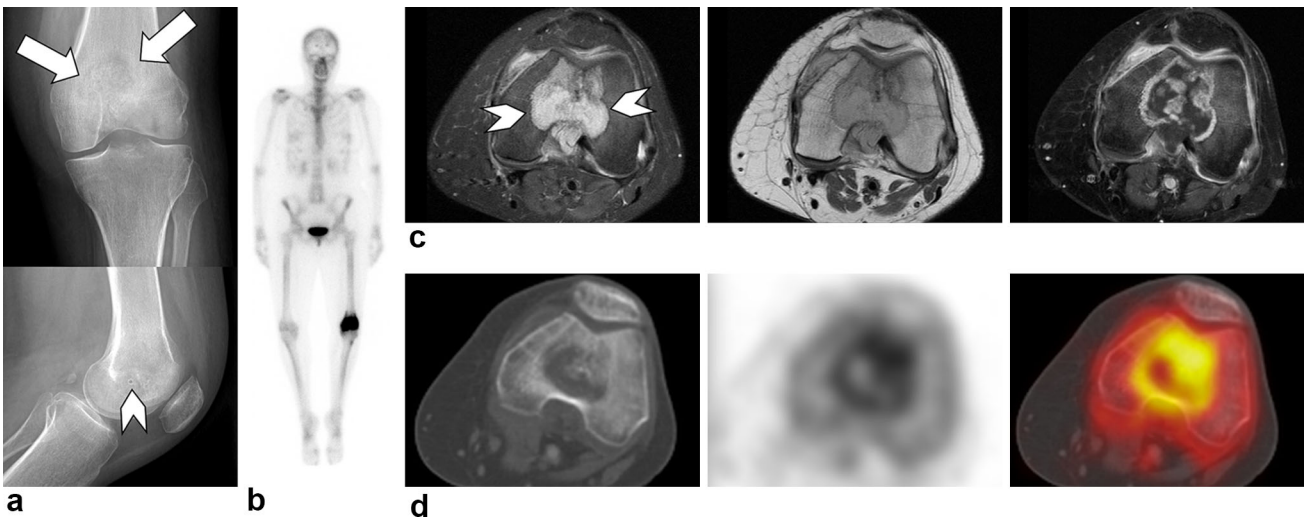

Fig. 7 A 53-year-old female suffering from left knee pain for a year diagnosed with a grade II chondrosarcoma. **a** AP and LL radiographs show an ill-defined distal femoral roughly oval-shaped lesion (*arrows*) in the distal femoral metaphysis. **b** Whole-body bone scan showing increased uptake at the level of the left knee; no metastatic foci are seen. **c** MRI (axial PD FS, T1w and T1w FS +C) demonstrating a lesion within the distal femur (*arrowheads*). The lesion is hyperintense on the fat-saturated sequence and presents heterogeneous enhancement after contrast media administration. **d** FDG PET/CT showing a destructive mixed lytic and sclerotic lesion within the distal femur associated with hypermetabolism

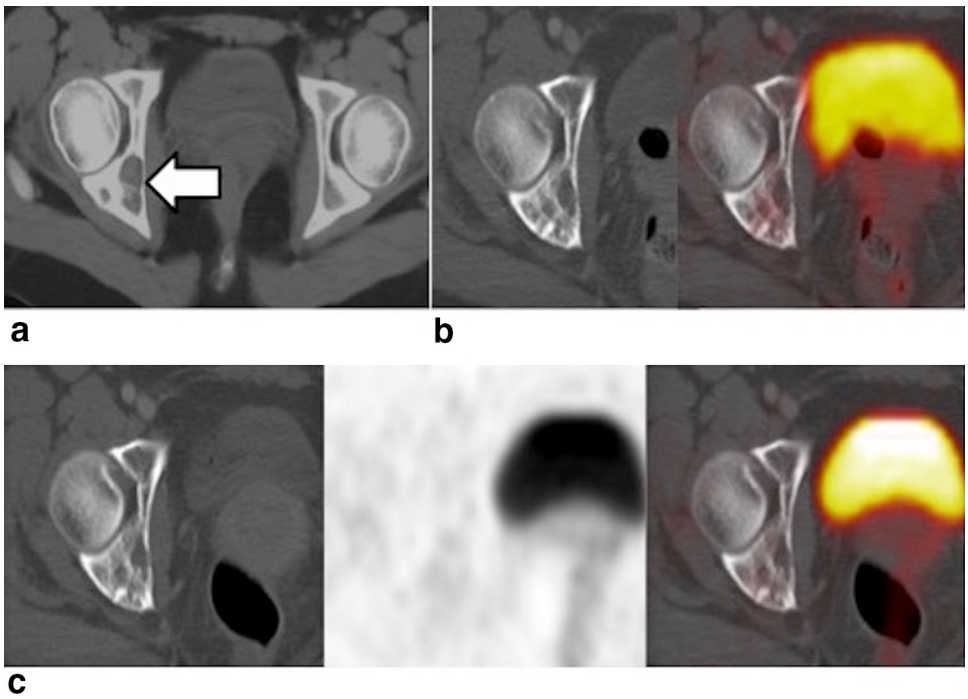

Fig. 8 A patient with history of Ollier's disease (multiple enchondromatosis). **a** CT image shows a multilobulated osteolytic lesion centered in the right acetabulum (*arrow*) with cortical thinning. Follow-up PET/CT studies obtained at 20 and 23 years are shown in images **b** and **c**, respectively. The lesion demonstrates low FDG avidity in both studies. The lack of increased metabolism and the stable appearance suggest against high-grade focal malignancy

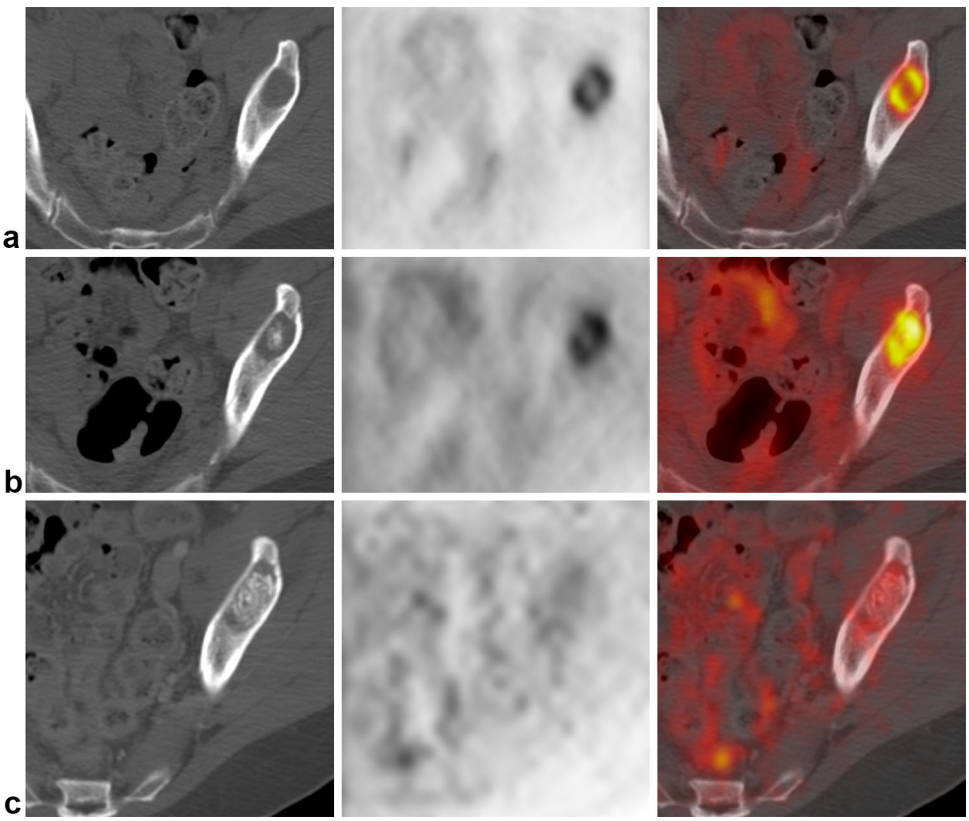

Fig. 9 A 39-year-old female suffering from mesenchymal chondrosarcoma of the left iliac wing. At baseline (**a**; axial CT, PET, PET/CT fused reconstruction), the lesion is predominantly lytic with intense FDG uptake. After 6 cycles of chemotherapy with doxorubicin, vincristine, and cytoxan (**b**), it appears to be more sclerotic. After adjuvant radiotherapy (**c**), the lesion is mostly sclerotic with low FDG uptake, likely to represent response to therapy

characterized by a mean SUVmax of 4.9, while malignant fibrous histiocytoma is associated with a significantly greater value (SUVmax of 27.1) [50, 51].

FD and other fibrous lesions such as non-ossifying fibroma and fibrous cortical defect can be misdiagnosed as metastatic cancer in the staging of other primary tumors as all of these entities can demonstrate elevated FDG uptake. There are multiple reports in the literature regarding bone lesions biopsied as suspected metastasis from sarcomas, squamous cell carcinoma, and breast cancer [52–54]

(Fig. 10). FD can be a potential pitfall also in case of 18F-NaF PET/CT: for example, the literature reports a case where an 18F-NaF-avid region of fibrous dysplasia was misdiagnosed as a metastasis in a patient suffering from breast cancer [55]. We recommend a close review of CT images and clinical history to avoid unnecessary biopsies and resulting false positives.

Bone Marrow Primary Bone Tumors

Multiple Myeloma

Multiple myeloma (MM) represents approximatively 1 % of all cancers and it is characterized by abnormal plasma cell accumulating in the bone marrow interfering with the normal hematopoiesis and often overproducing abnormal levels of immunoglobulin. Beyond clinical criteria based on blood, urine laboratory tests and bone marrow biopsy, imaging data are important to correctly diagnose and stage MM. The original Durie–Salmon staging system (1975) [56] included as an imaging technique only the bone survey; this technique has been demonstrated to have low sensitivity in detecting MM lesions, in that at least 30 % of the trabecular bone needs to be involved. More recently, different techniques including CT, MRI, and PET/CT have been studied in the assessment of MM [57–59]; CT is more sensitive than skeletal survey but suboptimal for intramedullary lesions or diffuse bone marrow involvement. MRI has been demonstrated to be the superior imaging modality for the detection of diffuse bone marrow involvement but suboptimal for extramedullary disease assessment. On the other hand, 18F-FDG PET/CT was demonstrated to be optimal for extramedullary disease assessment but suboptimal for bone marrow involvement and skull lesions [60, 61]. For these reasons, the Durie–Salmon classification was implemented with PET/CT and MRI criteria for the staging of MM. In the revised classification (Durie-Salmon plus 2006), the number of focal lesions and severity of diffuse disease was graded given their correlation with the clinical outcome. During staging, the number of 18F-FDG-avid lesions correlates with laboratory data and with shorter survival [62]. In addition, the presence of extramedullary disease significantly affects outcome (5-fold higher risk of progression) [60]. 18F-FDG PET/CT helps in treatment response assessment [63–65]; PET/CT is better than MRI in detecting persistency or recurrence of MM (Fig. 11). Furthermore, the semiquantitative values provided by FDG PET/CT correlate with prognosis; in particular, SUVs greater than 4.2 after induction therapy correlate with poor outcome, while a complete metabolic response correlates with a favorable outcome [66]. Comparison of SUVs between pre- and posttreatment scans shows change in disease activity; specifically, a decrease in SUV of lesions by at least 20 % has been correlated with better outcomes. Previous studies showed a complementary role for 18F-NaF in addition to 18F-FDG in the assessment of patients suffering from MM, but without any clear advantages [67–69].

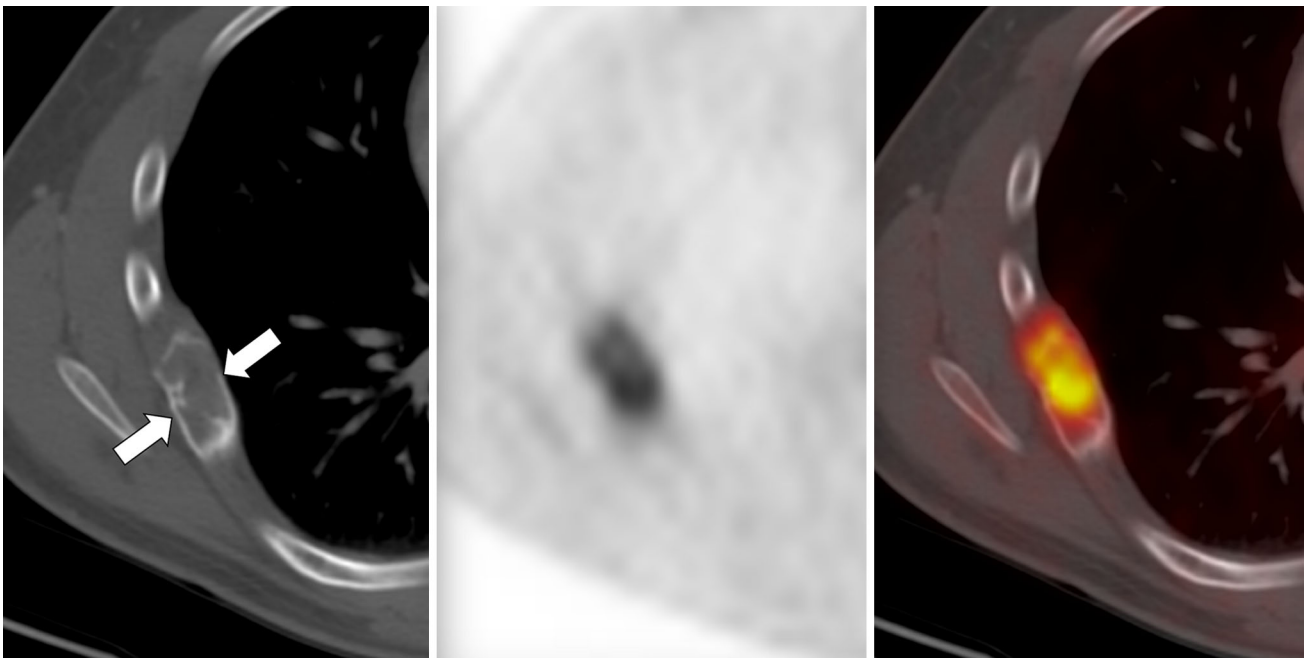

Fig. 10 A 21-year-old male with Hodgkin's lymphoma. 18F-FDG PET/CT study was obtained for staging. A predominantly lytic FDG-avid lesion of the 7th right rib (*arrows*) was interpreted as possible lymphoma localization. The lesion was biopsied and proven to be fibrous dysplasia. After chemotherapy (not shown), the lesion remained highly FDG avid

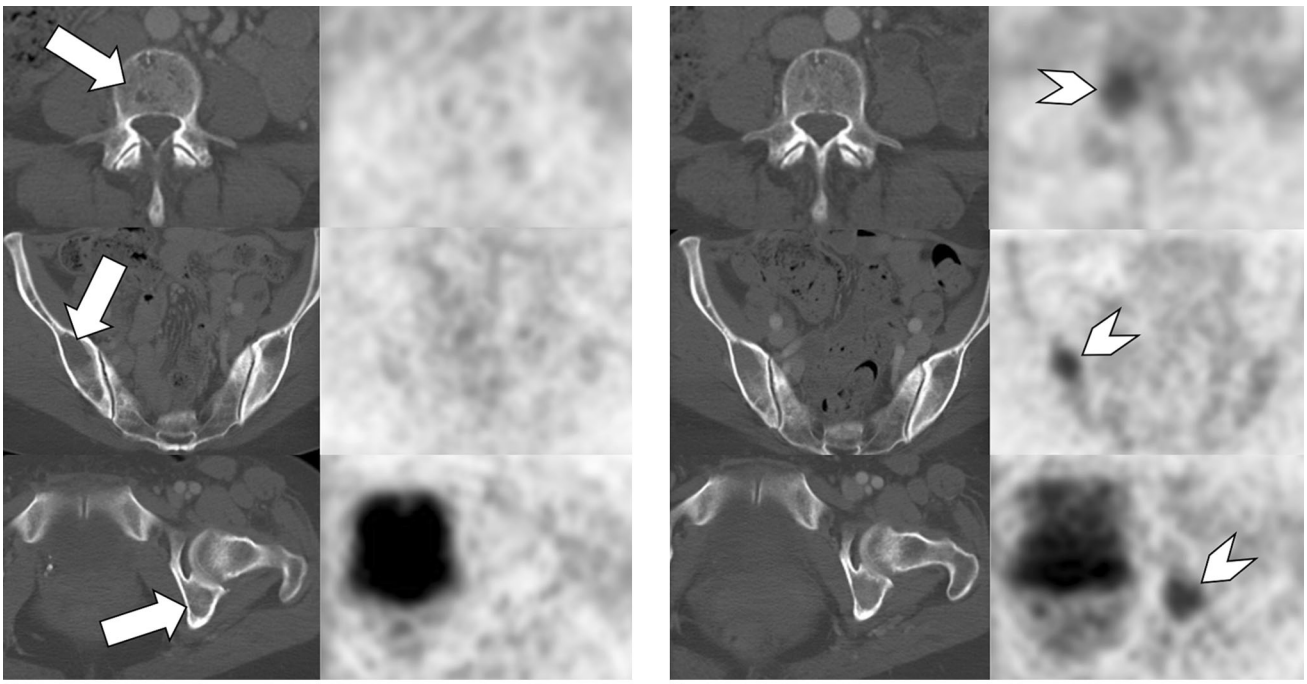

Fig. 11 A 51-year-old male suffering from IgG Kappa myeloma. The PET/CT study shows predominantly lytic lesions of L4 vertebral body, right posterior ilium, and the left ischium (*arrows*) without hypermetabolism above background (**a**). On the 2-year follow-up study (**b**), there has been an interval increase in FDG avidity (*arrowheads*) consistent with multiple myeloma reactivation

PET/CT also has a role in the diagnosis of monoclonal gammopathy of unknown significance (MGUS), smoldering myeloma, and plasmacytoma. The absence of 18F-FDG-avid lesions on PET/CT characterizes MGUS, while the presence of a single lesion can be seen in smoldering myeloma, indicating an increased risk for disease progression [63]. Plasmacytoma is often interpreted as early-stage MM with only one of the lesions detected. The disease can progress to MM, therefore PET/CT is warranted.

Primary Bone Lymphoma

Primary bone lymphomas are usually non-Hodgkin's lymphomas, with large B cell lymphoma the most common type. PET/CT is superior to cross-sectional imaging alone for the diagnosis, treatment response assessment, and evaluation of recurrence of lymphoma [70, 71].

As a staging technique, PET/CT shows increased 18F-FDG uptake at the level of the involved areas (Fig. 12). Different patterns of uptake can be seen: diffuse, focal or patchy, and heterogeneous. The use of PET/CT can have limited application in the setting of cytokine stimulation which causes diffuse increased uptake within the bone marrow spaces [72]. The use of FDG PET/CT in the assessment of treatment response is well established [73], and different grading systems for response assessment have been evaluated and used clinically [74–76]; for example, the Deauville score is one of the most utilized scales in treatment assessment. Early metabolic response to the therapy might change the therapy and possibly shorten the cycles of chemotherapy, thereby diminishing the long-term side effects [77].

Miscellaneous Tumors

Ewing Sarcoma

Ewing Sarcoma (ES) is the second most common malignant tumor in children and young adults. The first imaging modality in the assessment of Ewing sarcoma is always the plain film, which usually demonstrates a lesion in the diaphysis of a long bone, most commonly the femur. Local staging is then performed with MRI, and CT is used for evaluating for distant metastatic site, particularly within the lung. The most important prognostic factors in the staging of ES are the size of the lesion and distant metastases. PET/CT has been shown to be superior to MRI for skip lesions, especially in the active pediatric bone marrow [78], and in the detection of metastatic lymph nodes, but inferior to chest CT in the evaluation of pulmonary metastases [79–82]. Recently, several studies have focused on the value of 18F-FDG PET/CT in ES [83, 84]. The evaluation of pretreatment and posttreatment scans has been demonstrated to be useful in the characterization of the tumor and

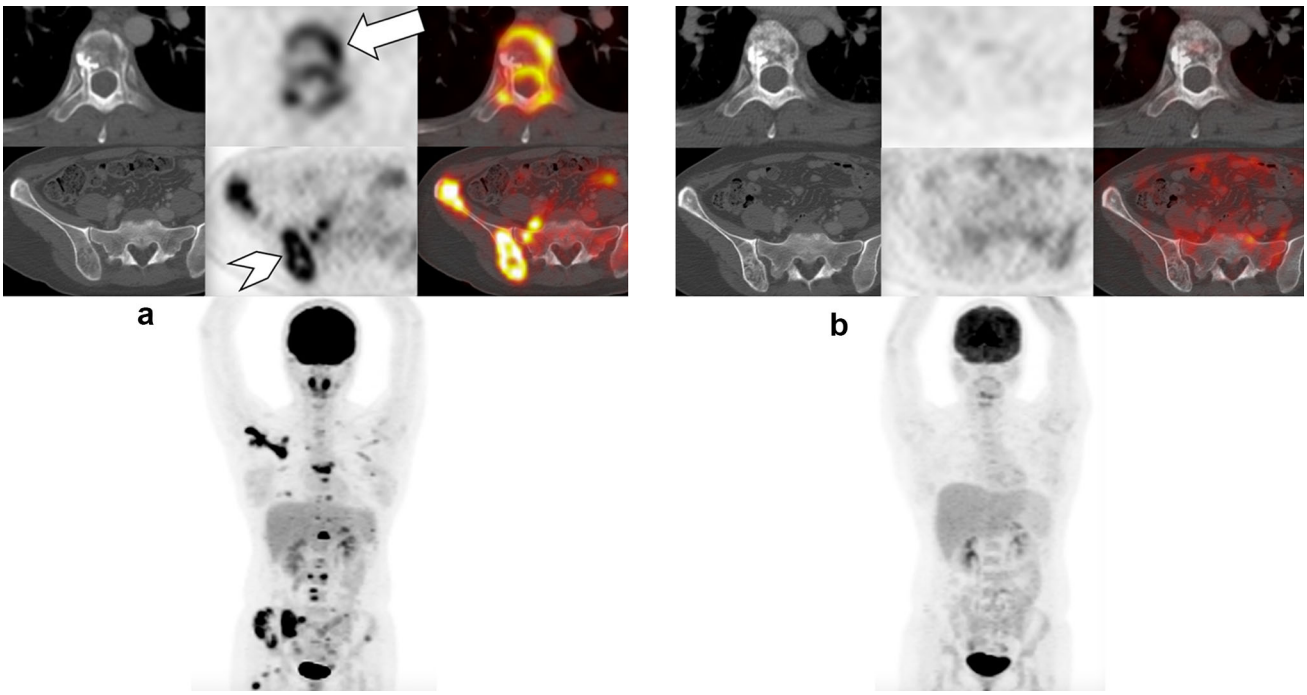

Fig. 12 A 28-year-old female suffering from primary osseous diffuse large B-cell lymphoma. **a** PET/CT study shows multiple intensely hypermetabolic lesions throughout the axial and proximal appendicular skeleton, including the right scapula, manubrium, bilateral ribs, thoracolumbar spine (T6 SUVmax 14.2; *white arrow*), bilateral iliac bone (right ilium SUVmax 15.8, *white arrowhead*), and right proximal femur. **b** After 4 months of chemotherapy (REPOCH), the follow-up study shows complete metabolic response

the therapy response [85–87] (Fig. 13). On the pretreatment scan, elevated SUV correlates with high-grade tumors and SUVmax greater than 5.8 correlates with poor prognosis [86, 88]; furthermore, post-neoadjuvant treatment SUVs less than 2.5 correlate with good histological response (>90 % necrosis) and longer survival [89].

Giant Cell Tumor

The giant cell tumor (GCT) is a common skeletal tumor, accounting for about 5 % of all primary osseous neoplasms, with 80 % of cases reported between the 2nd and the 5th decades [90, 91]. GCT arises following fusion of the growth plate, extending from the bone's metaphysis to the epiphysis. The most common site of GCT is the knee, involved in more than half of the cases. GCTs are generally benign tumors but might degenerate in sarcomas and rarely metastasize; therefore, they are often thought as quasi-malignant lesions.

On x-ray, the typical appearance of GCT is an expansile lesion without bone matrix at the level of metaphysis/epiphysis of a long bone is a hint, which suggests further assessment with CT and MRI. CT better evaluates the absence of mineralization, the narrow transition zone, and the cortical thinning with possible periosteal reaction, while MRI shows a typical whorled appearance on T2-weighted sequences and better detects the presence soft tissue extent. On PET/CT, GCTs are extremely 18F-FDG avid, with SUVs overlapping those of malignant bone tumors [41]. The uptake is often more prominent at the periphery with a central photopenic region (doughnut sign) (Fig. 14). The high vascularity of the tumor leads to a generalized regional hyperemia which can be seen as diffuse increased in radiotracer uptake [92].

In the rare case of multicentric giant cell tumors, the role of PET is to detect occult lesions, as it has been highlighted by Vaishya et al. [93] and 0'Connor et al. [94]. Rarely, GCT can metastasize or transform into malignant sarcomas: in this case, PET/CT is useful in detecting metastasis [95]. At the level of the primary malignancy, PET/CT can detect foci of more prominent uptake, which might be suitable for biopsy.

Pitfall

PET/CT is a very powerful tool in the assessment of bone malignancy; however, PET/CT findings can sometimes be difficult to interpret and lead to false-positive findings or produce additional work-up of benign entities.

There is a wide range of hypermetabolic lesions that are benign, but in the setting of the assessment of bone primary or metastatic tumors might be miscalled. Some of the most frequent benign hypermetabolic lesions are fibrous dysplasia, Paget's disease, abscess, and fractures. Paget's

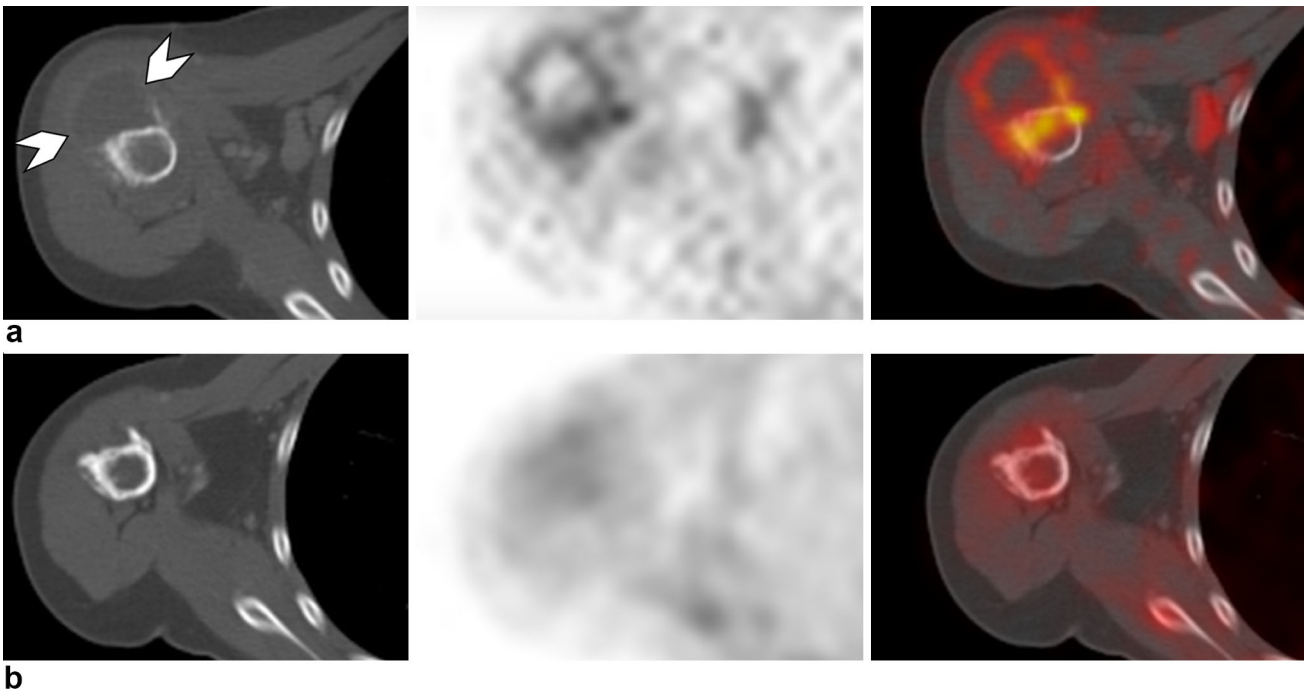

Fig. 13 A 12-year-old female suffering from Ewing's sarcoma of the right humerus. **a** PET/CT study shows the primary lesion (SUVmax of 7.0) within the right proximal humerus with associated cortical destruction and a significant soft tissue component (*arrowheads*). After 5 cycles of chemotherapy (**b**), there is an interval decrease in FDG avidity (SUVmax of 2.7) and almost complete resolution of the soft tissue mass. The patient continued chemotherapy and radiotherapy for lung metastases

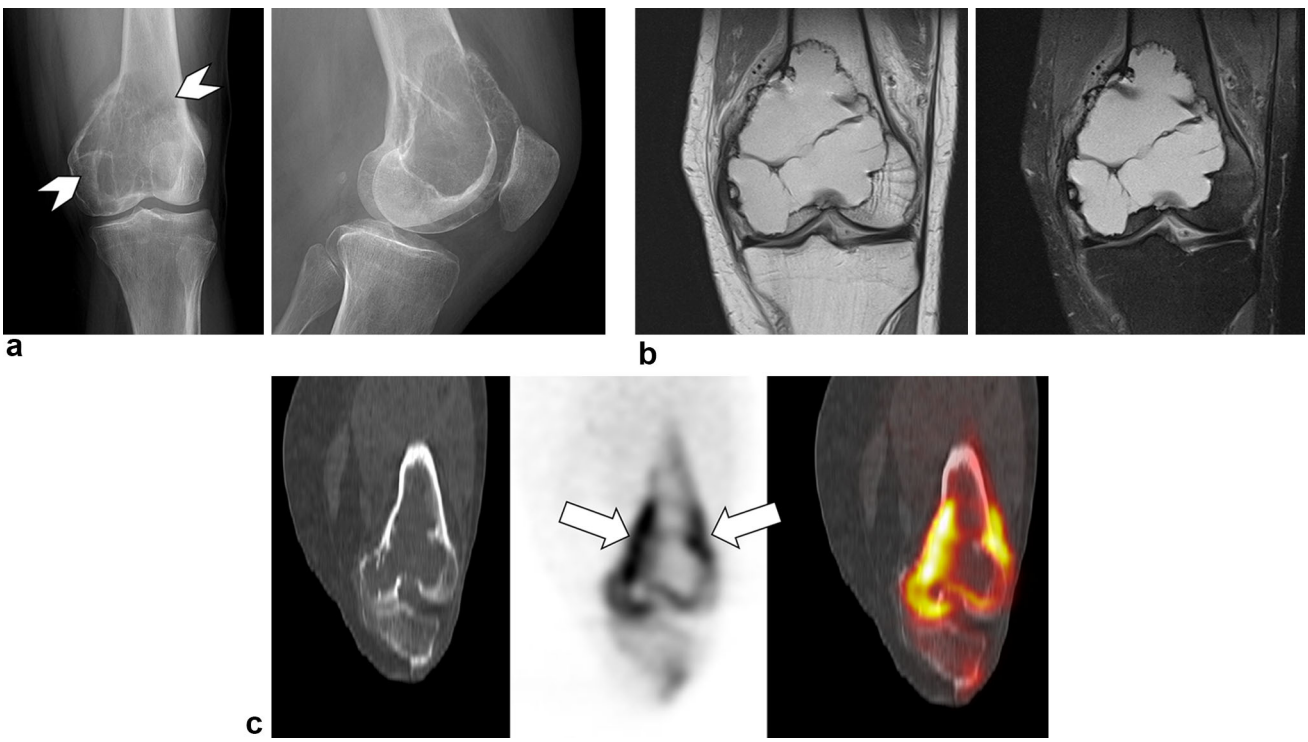

Fig. 14 A 57-year-old patient suffering from a giant cell tumor (GCT) of the left femur with secondary aneurysmal bone cyst. **a** AP and LL radiographs show an expansile, eccentrically located lucent lesion (*arrowheads*) with narrow zone of transition and non-sclerotic borders. The lesion extends from the closed physes into the epiphysis. **b** MRI (coronal T1w and PD FS sequences) demonstrating a multilobulated lesion with high signal intensity. **C** PET/CT study (coronal reformatted CT, PET, and PET/CT reconstructions) shows intense FDG avidity at the periphery of the lesion (*arrows*)

disease can be extremely hypermetabolic as well as intensely 18F-NaF avid on PET/CT images. Paget's has a typical whorled appearance with thinning of the trabecular bone and thickening of the cortical bone and can have lysis and sclerosis of mixed features. These features can resemble metastases as described in multiple reports in the literature [96, 97]. Often, abscess can be localized in the bone and might be in the differential diagnosis with eosinophilic granuloma or GCT.

Also fractures can be misinterpreted as malignancy, for example it is difficult to distinguish between a stress fracture and an osteoid osteoma.

Therefore, even if PET/CT is considered useful in the assessment of tumors, PET/CT is not always a straightforward tool without risks but presents also multiple challenges in interpretation, which need to be resolved by the radiologist using the combination of available clinical history and results of other imaging modalities.

Conclusions

PET/CT is a hybrid imaging technique increasingly used in the diagnosis, staging, and follow-up of primary bone neoplasms. The use of PET/CT in some malignancies such as lymphoma and multiple myeloma has been steadily established, while its role in work-up of other primary bone malignancies is still discussed. We believe that PET/CT can add valuable information in distinguishing benign from malignant lesions and in the staging of malignant bone tumors. Furthermore, PET/CT can play a role in biopsy planning, treatment planning, and response assessment.

Compliance with Ethical Guidelines

Conflict of interest Julio Brandao Guimaraes, Luca Facchetti, Leticia Rigo, Diego Lessa Garcia, Pricila Gama, and Lorenzo Nardo each declare no potential conflicts of interest. Benjamin L. Franc is a section editor for Current Radiology Reports.

Human and Animal Rights and Informed Consent This article does not contain any studies with human or animal subjects performed by any of the authors.

References

Papers of particular interest, published recently, have been highlighted as:
- • Of importance
- •• Of major importance

1. http://seer.cancer.gov/statfacts/html/bones.html.
2. NCI. SEER Cancer Statistics Review, 1975–2008. National Cancer Institute; 2011. http://www.sercancergov/csr/1975_2008/.
3. Liu F, Zhang Q, Zhu D, et al. Performance of positron emission tomography and positron emission tomography/computed tomography using Fluorine-18-Fluorodeoxyglucose for the diagnosis, staging, and recurrence assessment of bone sarcoma: a systematic review and meta-analysis. Medicine (Baltimore). 2015;94:e1462.
4. Bastiaannet E, Groen H, Jager PL, et al. The value of FDG-PET in the detection, grading and response to therapy of soft tissue and bone sarcomas; a systematic review and meta-analysis. Cancer Treat Rev. 2004;30:83–101.
5. ACR Appropriateness Criteria: Primary Bone Tumors. Date of origin: 1995 Last review date: 2015.
6. Charest M, Hickeson M, Lisbona R, Novales-Diaz JA, Derbekyan V, Turcotte RE. FDG PET/CT imaging in primary osseous and soft tissue sarcomas: a retrospective review of 212 cases. Eur J Nucl Med Mol Imaging. 2009;36:1944–51.
7. Fuglo HM, Jorgensen SM, Loft A, Hovgaard D, Petersen MM. The diagnostic and prognostic value of (1)(8)F-FDG PET/CT in the initial assessment of high-grade bone and soft tissue sarcoma. A retrospective study of 89 patients. Eur J Nucl Med Mol Imaging. 2012;39:1416–24.
8. • Byun BH, Kim SH, Lim SM et al: Prediction of response to neoadjuvant chemotherapy in osteosarcoma using dual-phase (18)F-FDG PET/CT. Eur Radiol. 2015;25:2015–24. *The dual-point PET/CT is a promising tool and the authors demonstrated that the histological response after neoadjuvant chemotherapy can be predicted by using the retention index (RI) at baseline.*
9. Tian R, Su M, Tian Y, et al. Dual-time point PET/CT with F-18 FDG for the differentiation of malignant and benign bone lesions. Skeletal Radiol. 2009;38:451–8.
10. Schillaci O. Use of dual-point fluorodeoxyglucose imaging to enhance sensitivity and specificity. Semin Nucl Med. 2012;42:267–80.
11. Yoon HJ, Kim SK, Kim TS, et al. New application of dual point 18F-FDG PET/CT in the evaluation of neoadjuvant chemoradiation response of locally advanced rectal cancer. Clin Nucl Med. 2013;38:7–12.
12. Minamimoto R, Mosci C, Jamali M, et al. Semiquantitative analysis of the biodistribution of the combined (1)(8)F-NaF and (1)(8)F-FDG administration for PET/CT imaging. J Nucl Med. 2015;56:688–94.
13. • Jackson T, Mosci C, von Eyben R et al. Combined 18F-NaF and 18F-FDG PET/CT in the evaluation of sarcoma patients. Clin Nucl Med. 2015;40:720–4. *The authors compared 18F-NaF PET/CT and 18F-FDG PET/CT in patients suffering from soft tissue sarcoma and bone sarcoma, enlightening the advantages of each techniques and the combination of both.*
14. Mirabello L, Troisi RJ, Savage SA. Osteosarcoma incidence and survival rates from 1973 to 2004: data from the surveillance, epidemiology, and end results program. Cancer. 2009;115:1531–43.
15. Resnick DKM, Greenway GD. Tumor and tumor-like lesions of bone: imaging and pathology of specific lesions. In: Resnick D, Kransdorf MJ, editors. Bone and joint imaging. Philadelphia: Elsevier Saunders; 2005. p. 1120–11.
16. Choi YY, Kim JY, Yang SO. PET/CT in benign and malignant musculoskeletal tumors and tumor-like conditions. Semin Musculoskelet Radiol. 2014;18:133–48.
17. Peller PJ. Role of positron emission tomography/computed tomography in bone malignancies. Radiol Clin North Am. 2013;51:845–64.
18. Quartuccio N, Treglia G, Salsano M, et al. The role of Fluorine-18-Fluorodeoxyglucose positron emission tomography in staging and restaging of patients with osteosarcoma. Radiol Oncol. 2013;47:97–102.

19. O'Sullivan PJ, Rohren EM, Madewell JE. Positron emission tomography-CT imaging in guiding musculoskeletal biopsy. Radiol Clin North Am. 2008;46:475–86, v.
20. Schulte M, Brecht-Krauss D, Heymer B, et al. Grading of tumors and tumorlike lesions of bone: evaluation by FDG PET. J Nucl Med. 2000;41:1695–701.
21. Tateishi U, Yamaguchi U, Seki K, Terauchi T, Arai Y, Kim EE. Bone and soft-tissue sarcoma: preoperative staging with fluorine 18 fluorodeoxyglucose PET/CT and conventional imaging. Radiology. 2007;245:839–47.
22. London K, Stege C, Cross S, et al. 18F-FDG PET/CT compared to conventional imaging modalities in pediatric primary bone tumors. Pediatr Radiol. 2012;42:418–30.
23. Hongtao L, Hui Z, Bingshun W, et al. 18F-FDG positron emission tomography for the assessment of histological response to neoadjuvant chemotherapy in osteosarcomas: a meta-analysis. Surg Oncol. 2012;21:e165–70.
24. Gaston LL, Di Bella C, Slavin J, Hicks RJ, Choong PF. 18F-FDG PET response to neoadjuvant chemotherapy for Ewing sarcoma and osteosarcoma are different. Skeletal Radiol. 2011;40:1007–15.
25. Costelloe CM, Chuang HH, Madewell JE. FDG PET/CT of primary bone tumors. AJR Am J Roentgenol. 2014;202:W521–31.
26. Cheon GJ, Kim MS, Lee JA, et al. Prediction model of chemotherapy response in osteosarcoma by 18F-FDG PET and MRI. J Nucl Med. 2009;50:1435–40.
27. Schirrmeister H, Guhlmann CA, Elsner K, et al. Positron emission tomography of the skeletal system using 18FNa: frequency, distribution and appearance of skeletal metastases. Rontgenpraxis. 1999;52:19–25.
28. Healey JH, Ghelman B. Osteoid osteoma and osteoblastoma. Current concepts and recent advances. Clin Orthop Relat Res. 1986;76–85.
29. Iyer RS, Chapman T, Chew FS. Pediatric bone imaging: diagnostic imaging of osteoid osteoma. AJR Am J Roentgenol. 2012;198:1039–52.
30. Kransdorf MJ, Stull MA, Gilkey FW, Moser RP Jr. Osteoid osteoma. Radiographics. 1991;11:671–96.
31. Saccomanni B. Osteoid osteoma and osteoblastoma of the spine: a review of the literature. Curr Rev Musculoskelet Med. 2009;2:65–7.
32. Chotel F, Franck F, Solla F, et al. Osteoid osteoma transformation into osteoblastoma: fact or fiction? Orthop Traumatol Surg Res. 2012;98:S98–104.
33. Al-Muqbel KM, Al-Omari MH, Audat ZA, Alqudah MA. Osteoblastoma is a metabolically active benign bone tumor on 18F-FDG PET imaging. J Nucl Med Technol. 2013;41:308–10.
34. Jeong YJ, Sohn MH, Lim ST, et al. Osteoblastoma in the nasal cavity: F-18 FDG PET/CT and Tc-99 m MDP 3-phase bone scan findings with pathologic correlation. Clin Nucl Med. 2011;36:214–7.
35. Kole AC, Nieweg OE, Hoekstra HJ, van Horn JR, Koops HS, Vaalburg W. Fluorine-18-fluorodeoxyglucose assessment of glucose metabolism in bone tumors. J Nucl Med. 1998;39:810–5.
36. Imperiale A, Moser T, Ben-Sellem D, Mertz L, Gangi A, Constantinesco A. Osteoblastoma and osteoid osteoma: morphofunctional characterization by MRI and dynamic F-18 FDG PET/CT before and after radiofrequency ablation. Clin Nucl Med. 2009;34:184–8.
37. Aoki J, Sone S, Fujioka F, et al. MR of enchondroma and chondrosarcoma: rings and arcs of Gd-DTPA enhancement. J Comput Assist Tomogr. 1991;15:1011–6.
38. Lee FY, Yu J, Chang SS, Fawwaz R, Parisien MV. Diagnostic value and limitations of fluorine-18 fluorodeoxyglucose positron emission tomography for cartilaginous tumors of bone. J Bone Joint Surg Am. 2004;86-A:2677–85.
39. Feldman F, Van Heertum R, Saxena C, Parisien M. 18FDG-PET applications for cartilage neoplasms. Skeletal Radiol. 2005;34:367–74.
40. Aoki J, Watanabe H, Shinozaki T, Tokunaga M, Inoue T, Endo K. FDG-PET in differential diagnosis and grading of chondrosarcomas. J Comput Assist Tomogr. 1999;23:603–8.
41. Aoki J, Watanabe H, Shinozaki T, et al. FDG PET of primary benign and malignant bone tumors: standardized uptake value in 52 lesions. Radiology. 2001;219:774–7.
42. Boyce AM, Collins MT. Fibrous dysplasia/mccune-albright syndrome. In: Pagon RA, Adam MP, Ardinger HH et al, editors. GeneReviews(R), Seattle (WA); 1993.
43. Kransdorf MJ, Moser RP Jr, Gilkey FW. Fibrous dysplasia. Radiographics. 1990;10:519–37.
44. Fitzpatrick KA, Taljanovic MS, Speer DP, et al. Imaging findings of fibrous dysplasia with histopathologic and intraoperative correlation. AJR Am J Roentgenol. 2004;182:1389–98.
45. D'Souza MM, Jaimini A, Khurana A, et al. Polyostotic fibrous dysplasia on F-18 FDG PET/CT imaging. Clin Nucl Med. 2009;34:359–61.
46. Saxon PH, Scalcione LR, Luongo JA, et al. McCune-albright syndrome: intensely hypermetabolic polyostotic fibrous dysplasia on F-18 FDG-PET. Clin Nucl Med. 2009;34:795–7.
47. Case DB, Chapman CN Jr, Freeman JK, Polga JP. Best cases from the AFIP: a typical presentation of polyostotic fibrous dysplasia with myxoma (Mazabraud syndrome). Radiographics. 2010;30:827–32.
48. Berrebi O, Steiner C, Keller A, Rougemont AL, Ratib O. F-18 fluorodeoxyglucose (FDG) PET in the diagnosis of malignant transformation of fibrous dysplasia in the pelvic bones. Clin Nucl Med. 2008;33:469–71.
49. Qu N, Yao W, Cui X, Zhang H. Malignant transformation in monostotic fibrous dysplasia: clinical features, imaging features, outcomes in 10 patients, and review. Medicine (Baltimore). 2015;94:e369.
50. Shin DS, Shon OJ, Han DS, Choi JH, Chun KA, Cho IH. The clinical efficacy of (18)F-FDG-PET/CT in benign and malignant musculoskeletal tumors. Ann Nucl Med. 2008;22:603–9.
51. Ho L, Meka M, Gamble BK, Shim JJ, Seto J. Left maxillary sinus malignant fibrous histiocytoma on FDG PET-CT. Clin Nucl Med. 2009;34:967–8.
52. Strobel K, Exner UE, Stumpe KD, et al. The additional value of CT images interpretation in the differential diagnosis of benign vs. malignant primary bone lesions with 18F-FDG-PET/CT. Eur J Nucl Med Mol Imaging. 2008;35:2000–8.
53. Guler I, Nayman A, Gedik GK, Koplay M, Sari O. Fibrous dysplasia mimicking vertebral bone metastasis on 18F-FDG PET/computed tomography in a patient with tongue cancer. Spine J. 2015;15:1501–2.
54. Suman Kc S, Sharma P, Singh H, Bal C, Kumar R. Fibrous dysplasia mimicking bone metastasis on both bone scintigraphy and (18)F-FDG PET-CT: diagnostic dilemma in a patient with breast cancer. Nucl Med Mol Imaging. 2012;46:318–9.
55. Lee H, Lee KS, Lee WW. 18F-NaF PET/CT findings in fibrous dysplasia. Clin Nucl Med. 2015;40:912–4.
56. Durie BG, Salmon SE. A clinical staging system for multiple myeloma. Correlation of measured myeloma cell mass with presenting clinical features, response to treatment, and survival. Cancer. 1975;36:842–54.
57. Dimopoulos M, Terpos E, Comenzo RL, et al. International myeloma working group consensus statement and guidelines regarding the current role of imaging techniques in the diagnosis and monitoring of multiple Myeloma. Leukemia. 2009;23:1545–56.
58. Durie BG, Kyle RA, Belch A, et al. Myeloma management guidelines: a consensus report from the scientific advisors of the International Myeloma Foundation. Hematol J. 2003;4:379–98.
59. International Myeloma Working G. Criteria for the classification of monoclonal gammopathies, multiple myeloma and related

disorders: a report of the International Myeloma Working Group. Br J Haematol. 2003;121:749–57.
60. Zamagni E, Patriarca F, Nanni C, et al. Prognostic relevance of 18-F FDG PET/CT in newly diagnosed multiple myeloma patients treated with up-front autologous transplantation. Blood. 2011;118:5989–95.
61. Agarwal A, Chirindel A, Shah BA, Subramaniam RM. Evolving role of FDG PET/CT in multiple myeloma imaging and management. AJR Am J Roentgenol. 2013;200:884–90.
62. Bartel TB, Haessler J, Brown TL, et al. F18-fluorodeoxyglucose positron emission tomography in the context of other imaging techniques and prognostic factors in multiple myeloma. Blood. 2009;114:2068–76.
63. Durie BG, Waxman AD, D'Agnolo A, Williams CM. Whole-body (18)F-FDG PET identifies high-risk myeloma. J Nucl Med. 2002;43:1457–63.
64. Schirrmeister H, Bommer M, Buck AK, et al. Initial results in the assessment of multiple myeloma using 18F-FDG PET. Eur J Nucl Med Mol Imaging. 2002;29:361–6.
65. Caldarella C, Isgro MA, Treglia I, Treglia G. Is fluorine-18-fluorodeoxyglucose positron emission tomography useful in monitoring the response to treatment in patients with multiple myeloma? Int J Hematol. 2012;96:685–91.
66. Park S, Lee SJ, Chang WJ, et al. Positive correlation between baseline PET or PET/CT findings and clinical parameters in multiple myeloma patients. Acta Haematol. 2014;131:193–9.
67. Sachpekidis C, Goldschmidt H, Hose D, et al. PET/CT studies of multiple myeloma using (18) F-FDG and (18) F-NaF: comparison of distribution patterns and tracers' pharmacokinetics. Eur J Nucl Med Mol Imaging. 2014;41:1343–53.
68. Ak I, Onner H, Akay OM. Is there any complimentary role of F-18 NaF PET/CT in detecting of osseous involvement of multiple myeloma? A comparative study for F-18 FDG PET/CT and F-18 FDG NaF PET/CT. Ann Hematol. 2015;94:1567–75.
69. Xu F, Liu F, Pastakia B. Different lesions revealed by 18F-FDG PET/CT and 18F-NaF PET/CT in patients with multiple myeloma. Clin Nucl Med. 2014;39:e407–9.
70. Park YH, Kim S, Choi SJ, et al. Clinical impact of whole-body FDG-PET for evaluation of response and therapeutic decision-making of primary lymphoma of bone. Ann Oncol. 2005;16:1401–2.
71. Cheson BD, Fisher RI, Barrington SF, et al. Recommendations for initial evaluation, staging, and response assessment of Hodgkin and non-Hodgkin lymphoma: the Lugano classification. J Clin Oncol. 2014;32:3059–68.
72. Yang YQ, Ding CY, Xu J, et al. Exploring the role of bone marrow increased FDG uptake on PET/CT in patients with lymphoma-associated hemophagocytic lymphohistiocytosis: a reflection of bone marrow involvement or cytokine storm? Leuk Lymphoma. 2015;. doi:10.3109/10428194.2015.1048442:1-8.
73. Moskowitz CH. Interim PET-CT in the management of diffuse large B-cell lymphoma. Hematology Am Soc Hematol Educ Program. 2012;2012:397–401.
74. Hutchings M, Barrington SF. PET/CT for therapy response assessment in lymphoma. J Nucl Med. 2009;50(Suppl 1):21S–30S.
75. Biggi A, Gallamini A, Chauvie S, et al. International validation study for interim PET in ABVD-treated, advanced-stage hodgkin lymphoma: interpretation criteria and concordance rate among reviewers. J Nucl Med. 2013;54:683–90.
76. Meignan M, Gallamini A, Meignan M, Gallamini A, Haioun C. Report on the first international workshop on interim-PET-scan in lymphoma. Leuk Lymphoma. 2009;50:1257–60.
77. Kasamon YL, Wahl RL. FDG PET and risk-adapted therapy in Hodgkin's and non-Hodgkin's lymphoma. Curr Opin Oncol. 2008;20:206–19.
78. Brenner W, Bohuslavizki KH, Eary JF. PET imaging of osteosarcoma. J Nucl Med. 2003;44:930–42.
79. Furth C, Amthauer H, Denecke T, Ruf J, Henze G, Gutberlet M. Impact of whole-body MRI and FDG-PET on staging and assessment of therapy response in a patient with Ewing sarcoma. Pediatr Blood Cancer. 2006;47:607–11.
80. Franzius C, Daldrup-Link HE, Sciuk J, et al. FDG-PET for detection of pulmonary metastases from malignant primary bone tumors: comparison with spiral CT. Ann Oncol. 2001;12:479–86.
81. Volker T, Denecke T, Steffen I, et al. Positron emission tomography for staging of pediatric sarcoma patients: results of a prospective multicenter trial. J Clin Oncol. 2007;25:5435–41.
82. McCarville MB, Christie R, Daw NC, Spunt SL, Kaste SC. PET/CT in the evaluation of childhood sarcomas. AJR Am J Roentgenol. 2005;184:1293–304.
83. Franzius C, Sciuk J, Brinkschmidt C, Jurgens H, Schober O. Evaluation of chemotherapy response in primary bone tumors with F-18 FDG positron emission tomography compared with histologically assessed tumor necrosis. Clin Nucl Med. 2000;25:874–81.
84. Bredella MA, Caputo GR, Steinbach LS. Value of FDG positron emission tomography in conjunction with MR imaging for evaluating therapy response in patients with musculoskeletal sarcomas. AJR Am J Roentgenol. 2002;179:1145–50.
85. O JH, Luber BS, Leal JP et al. Response to early treatment evaluated with 18F-FDG PET and PERCIST 1.0 predicts survival in patients with Ewing sarcoma family of tumors treated with a monoclonal antibody to the insulin-like growth factor 1 receptor. J Nucl Med. 2016. doi:10.2967/jnumed.115.162412.
86. Eary JF, Conrad EU, Bruckner JD, et al. Quantitative [F-18]fluorodeoxyglucose positron emission tomography in pretreatment and grading of sarcoma. Clin Cancer Res. 1998;4:1215–20.
87. Raciborska A, Bilska K, Drabko K, et al. Response to chemotherapy estimates by FDG PET is an important prognostic factor in patients with Ewing sarcoma. Clin Transl Oncol. 2016;18:189–95.
88. Hwang JP, Lim I, Kong CB, et al. Prognostic value of SUVmax measured by pretreatment Fluorine-18 fluorodeoxyglucose positron emission tomography/computed tomography in patients with ewing sarcoma. PLoS ONE. 2016;11:e0153281.
89. Hawkins DS, Schuetze SM, Butrynski JE, et al. [18F]Fluorodeoxyglucose positron emission tomography predicts outcome for Ewing sarcoma family of tumors. J Clin Oncol. 2005;23:8828–34.
90. Manaster BJ, Doyle AJ. Giant cell tumors of bone. Radiol Clin North Am. 1993;31:299–323.
91. Murphey MD, Nomikos GC, Flemming DJ, Gannon FH, Temple HT, Kransdorf MJ. From the archives of AFIP. Imaging of giant cell tumor and giant cell reparative granuloma of bone: radiologic-pathologic correlation. Radiographics. 2001;21:1283–309.
92. Strauss LG, Dimitrakopoulou-Strauss A, Koczan D, et al. 18F-FDG kinetics and gene expression in giant cell tumors. J Nucl Med. 2004;45:1528–35.
93. Vaishya R, Agarwal AK, Vijay V, Vaish A. Metachronous multicentric giant cell tumour in a young woman. BMJ Case Rep 2015; 2015.
94. O'Connor W, Quintana M, Smith S, Willis M, Renner J. The hypermetabolic giant: 18F-FDG avid giant cell tumor identified on PET-CT. J Radiol Case Rep. 2014;8:27–38.
95. Zhang Y, Reeve IP, Lewis DH. A case of giant cell tumor of sacrum with unusual pulmonary metastases: CT and FDG PET findings. Clin Nucl Med. 2012;37:920–1.
96. Kamaleshwaran KK, Natarajan S, Shibu D, Malaikkal A, Shinto AS. Paget's disease of pelvis mimicking metastasis in a patient with lung cancer evaluated using staging and follow-up imaging with fluorine-18 fluorodeoxyglucose-positron emission tomography/computed tomography. Indian J Nucl Med. 2015;30:151–3.
97. Mahmood S, Martinez de Llano SR. Paget disease of the humerus mimicking metastatic disease in a patient with metastatic malignant mesothelioma on whole body F-18 FDG PET/CT. Clin Nucl Med. 2008;33:510–2.